Simulations and generalized model of the effect of filler size dispersity on electrical percolation in rod networks

Citation: Mutiso, Rose M., Michelle C. Sherrott, Ju Li, and Karen I. Winey. "Simulations and Generalized Model of the Effect of Filler Size Dispersity on Electrical Percolation in Rod Networks." Phys. Rev. B 86, no. 21 (December 2012). © 2012 American Physical Society

As Published: http://dx.doi.org/10.1103/PhysRevB.86.214306

Publisher: American Physical Society

Persistent URL: http://hdl.handle.net/1721.1/95875

Version: Final published version: final published article, as it appeared in a journal, conference proceedings, or other formally published context

Simulations and generalized model of the effect of filler size dispersity on electrical percolation in rod networks

Rose M. Mutiso,[1] Michelle C. Sherrott,[1] Ju Li,[2] and Karen I. Winey[1]
[1]*Department of Materials Science and Engineering, University of Pennsylvania, Philadelphia, Pennsylvania 19146*
[2]*Department of Nuclear Science and Engineering and Department of Materials Science and Engineering, Massachusetts Institute of Technology, Cambridge, Massachusetts 02139*
(Received 17 July 2012; published 26 December 2012; corrected 3 January 2013)

We present a three-dimensional simulation of electrical conductivity in isotropic, polydisperse rod networks from which we determine the percolation threshold (ϕ_c). Existing analytical models that account for size dispersity are formulated in the slender-rod limit and are less accurate for predicting ϕ_c in composites with rods of modest L/D. Using empirical approximations from our simulation data, we generalized the excluded volume percolation model to account for both finite L/D and size dispersity, providing a solution for ϕ_c of polydisperse rod networks that is quantitatively accurate across the entire L/D range.

DOI: 10.1103/PhysRevB.86.214306 PACS number(s): 64.60.ah, 72.80.Tm

I. INTRODUCTION

Percolation theory describes connectivity of objects within a network structure and the effects of this connectivity on the macroscale properties of the system. Computational and analytical studies addressing the percolation of rods are important for predicting insulator–conductor transitions in composites with conductive particles. Such systems include early fiber-reinforced polymer composites and the more recent nanocomposites containing carbon nanotubes (CNTs), metal nanowires, and graphene that have sparked considerable interest because of dramatic improvement of the electrical properties of insulating polymers at very low filler concentrations (<1 vol% in some cases). Realizing the full potential of these novel materials requires an in-depth understanding and predictive capability of the key structure–property relationships, particularly geometric percolation.

Since the early 1980s, extensive analytical and computational studies of percolation phenomena have been conducted for sticks in two dimensions[1–3] and rods in three-dimensions.[4–11] Despite this large body of theoretical literature, there are major gaps in our understanding of the effects of experimentally typical non-idealities in polymer nanocomposites on the percolation threshold (ϕ_c) such as non-uniform filler dispersion and polydispersity in filler size, shape, and properties. Indeed these factors are believed to be a major source of the considerable disparity in the thresholds and conductivities reported in the literature for seemingly similar nanoparticle/polymer systems.[12] This is particularly true for carbon nanotubes, for which all synthesis methods yield nanotubes with varying diameter, length, and chirality. As the percolation phenomena are strongly dependent on the aspect ratio of the filler, wide distributions in filler length and diameter are expected to significantly affect the percolation threshold of the final composite. Recent analytical work by van der Schoot and coworkers[13–15] investigated the impact of polydisperse fillers using both percolation and liquid state theories, reporting a very strong sensitivity of ϕ_c on the degree of filler size dispersity. Chatterjee[16,17] employed a modified Bethe lattice approach to estimate ϕ_c of polydisperse rod networks, obtaining results that are consistent with Otten and van der Schoot's connectedness Ornstein–Zernike equation approach.[14,15] However, these analytical approaches employ approximations that are mean-field in nature, and can only be considered quantitatively accurate in the limit of very large aspect ratios ($L/D \to \infty$). Berhan and Sastry[5] showed that convergence to the slender-rod limit solution for monodisperse rod networks is very slow and not achieved for L/D as high as 500. Many important nanofillers have modest aspect ratios (<100), and common composite processing techniques such as sonication lead to dramatic size reduction for high-L/D fillers, such as CNTs.[18] Thus, the appropriateness and practical utility of existing slender-rod-limit theories when predicting percolation thresholds in particle networks and nanocomposites must be considered.

In this paper, we present a simulation study of the effect of filler size dispersity on the percolation threshold in three-dimensional isotropic networks containing finite-sized, conductive cylinders with modest aspect ratios ($L/D = 10-100$). We have previously used this simulation approach to explore the effects of orientation and aspect ratio on the electrical properties of polymer nanocomposites with monodisperse fillers.[10,11] In the latter study, our simulations successfully predicted experimental ϕ_c for silver nanowire–polystyrene composites with modest nanowire aspect ratios ($L/D < 35$). Furthermore, using empirical approximations from our simulation data, we will successfully generalize the widely used excluded volume model[4] for percolation in soft-core, monodisperse rod networks to account for finite L/D and size dispersity of rods. Our solution holds for arbitrary distributions in L and D, assuming that the distributions are independent, and provides quantitatively accurate ϕ_c predictions across the entire L/D range. Additionally, we adapt Otten and van der Schoot's slender-rod-limit analytical solution[14,15] to extend its applicability to polydisperse networks of finite-L/D rods. Our simulation results, coupled with our adaptations of existing analytical models, provide a robust and convenient predictive toolkit for composite design and evaluation.

II. SIMULATION METHOD

A random configuration of straight, soft-core (i.e., interpenetrable), cylindrical rods is generated in a large supercell

($h = 1$ unit, $l = \sqrt{0.1}$ unit, and $w = \sqrt{0.1}$ unit). In this paper, the centers of mass of the rods are randomly distributed in the supercell, and the angular distributions of the rod axes are uniformly random to form isotropic networks. For the first example of size dispersity, the rod lengths and diameters are normally distributed about a specified L_{mode} and D_{mode}, with the width of each length and diameter distribution (standard deviation, σ_L and σ_D) expressed as 0%−100% of the respective modes. In the second example of size dispersity, we simulate networks comprising two monodisperse size populations of low- and high-aspect-ratio rods. Here, low-aspect-ratio reference rods with $L/D = 10$ ($L = 0.04$ unit, $D = 0.004$ unit) are mixed with various fractions of longer (bidisperse distribution in rod length) or thinner (bidisperse distribution in rod diameter) rods with $L/D = 20$, 40, and 80 in the simulation volume.

The supercell is divided into tiling cubic sub-blocks, whose length is greater than the rod length, and rods that fall into each sub-block are registered. Aided by the sub-block data structures, the possible neighbors of each rod are determined with computational complexity that scales linearly with the total number of rods. Then, the shortest distance between the centers of two possible neighboring rods is calculated using a close-formed formula, from which one can determine whether they are in contact when this shortest distance is $<D$. A clustering analysis is then carried out to decompose the rod configuration into (i) percolating clusters of contacting rods that simultaneously touch the top and bottom surfaces of the supercell and (ii) non-percolating clusters. The total conductance is the sum of the individual percolating cluster conductances, and the non-percolating clusters are simply ignored. For each percolating cluster, one assumes every rod i has a uniform voltage V_i (no internal resistance) that is an unknown variable, except for those rods that touch the top ($V_i = 1$) or the bottom ($V_i = 0$). A system of linear equations is then established for each cluster, assuming that all the electrical resistance results from contact resistances between neighboring rods (contact resistance = 1 Ω, rod resistance = 0 Ω, matrix resistance = ∞), and the sum of electrical currents that flow in and out of any rod (that is not touching the top or bottom surface) must be zero. This system of linear equations is solved using the pre-conditioned conjugate gradient iterative (KSPCG) method[19] as implemented in the Portable, Extensible Toolkit for Scientific Computation (PETSc) package, where the incomplete LU factorization preconditioner (PCILU) is used, to obtain the cluster conductance. This procedure is repeated to generate a large number of configurations to obtain the ensemble-averaged conductance. Simulations were performed for each condition at a range of rod volume fractions (ϕ), corresponding to ∼2000–1,000,000 rods depending on the prescribed ϕ and L/D. For each case, the simulated conductivity was fit using a power law to obtain ϕ_c and the exponent t, and in all cases $t \approx 2$, the expected value for rods in three dimensions (see Supplemental Material Fig. 1).[20] In addition to finding ϕ_c, our simulation method predicts the conductivity at $\phi > \phi_c$, which we have previously used to study the effect of orientation.[10]

The assumptions underlying our simulations of rod networks and their implications are summarized here:

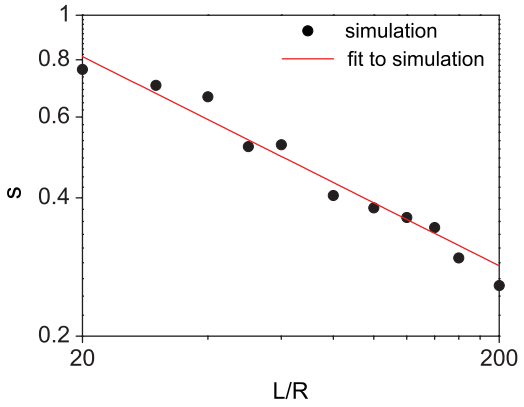

FIG. 1. (Color online) $\ln(s)$ vs $\ln(L/R)$ fit gives an empirical expression for s as a function of L/R [Eq. (6)].

(1) Soft-core (or interpenetrable) rods: Rods are allowed to overlap and are considered to be in contact when the shortest distance between their centers is less than D. While this is an unphysical assumption, our previous results show that it introduces negligible error,[11] particularly at higher aspect ratios when the overlap volume is small relative to the total rod volume.[8]

(2) Contact resistance ≫ rod resistance: Contact resistance dominates the electrical conductivity in polymer nanocomposites with conductive fillers, wherein electrons tunnel from one rod to the next across a polymer barrier.

(3) Contact resistance is fixed: While the contact resistance is a strong function of the inter-rod distances due to tunneling, substituting a step function by implementing a constant contact resistance is reliable.[11] Furthermore, an arbitrary constant value of the contact resistance (1 Ω) is sufficient to qualitatively capture experimental trends in the simulated conductivity.[10]

Points (1) and (3) are consistent with the tunneling percolation model proposed by Balberg and coworkers.[21–25] Here, the tunneling conductance of particles separated by a distance larger than the typical tunneling range is considered negligible, and these connections are essentially "removed" from the tunneling network (contact resistance = ∞). Thus, the observed conformity of experimental systems to geometric percolation theory arises from the percolation-like tunneling network of particles that have neighbors separated by distances of the order of the tunneling decay distance or less.

III. RESULTS AND DISCUSSION

In the widely used excluded volume model,[4] ϕ_c is determined by the excluded volume of the filler particles, rather than their true volume, where the excluded volume is defined as the volume surrounding a particle into which the center of mass of a second, identical, but differently oriented particle cannot enter without contacting the first particle. Specifically, the critical number of filler particles per unit volume required for geometrical percolation, N_c, is inversely proportional to the average excluded volume of a filler particle, $V_{\text{ex\_rod}}$:

$$N_c \propto \frac{1}{V_{\text{ex\_rod}}} \tag{1}$$

In the slender-rod limit ($L/D \to \infty$), it has been shown, using a cluster expansion method,[6,7] that this proportionality becomes a true equality. The average excluded per rod in a randomly oriented system of soft-core, cylindrical rods is given by[26]

$$V_{\text{ex\_rod}} = \frac{\pi}{2} D\left[\frac{\pi}{4} D^2 + L^2\right] + \frac{\pi}{4} D^2 L(3+\pi), \qquad (2)$$

where L and D are the length and diameter of the cylinder, respectively. Note that Eq. (2) for cylindrical rods is more appropriate for our simulations and experiments than the approximation based on the excluded volume of a sphero-(end-capped) cylinder that we have used previously.[10,11] Thus, the percolation threshold for an isotropic network of monodisperse cylindrical particles is given by:

$$\begin{aligned}\phi_c = N_c V_{\text{rod}} &= \frac{V_{\text{rod}}}{V_{\text{ex\_rod}}} \\ &= \frac{\frac{\pi}{4} D^2 L}{\frac{\pi}{2} D\left[\frac{\pi}{4} D^2 + L^2\right] + \frac{\pi}{4} D^2 L\,(3+\pi)} \\ &= \frac{1}{\frac{\pi}{2}\frac{D}{L} + 2\frac{L}{D} + (3+\pi)}, \end{aligned} \qquad (3)$$

where $V_{\text{rod}} = (\pi/4) D^2 L$ is the volume of a cylinder. Equation (3) predicts a decrease in ϕ_c with increasing rod aspect ratio, which is consistent qualitatively with experiments and simulations.

An underlying assumption of infinite aspect ratio makes Eq. (3) most appropriate for fillers with very high aspect ratios because the percolation threshold in a three-dimensional isotropic rod system has higher order dependencies on R/L that vanish in the slender-rod limit.[6,7] Néda *et al.*[9] conducted Monte Carlo simulations of isotropic, three-dimensional, soft-core rod networks and used their simulation data to derive a relationship between N_c and $V_{\text{ex\_rod}}$ that gives a numerical approximation of the constant of proportionality in Eq. (1) as a function of the rod aspect ratio. They introduced a variable s such that

$$s = N_c V_{\text{ex\_rod}} - 1, \qquad (4)$$

where N_c is extracted directly from their simulations. Their results confirmed the analytical prediction that $s = 0$ in the limit of $R/L \to 0$ and demonstrated that $\ln(s)$ varies linearly with $\ln(R/L)$. Berhan and Sastry[5] calculated s values from their Monte Carlo simulations for L/D ranging between 15 and 500, showing very slow convergence of s to the slender-rod limit value of 0.

Thus, a more appropriate analytical solution for the percolation threshold for isotropic, monodisperse rods with finite L/D is

$$\begin{aligned}\phi_c = N_c V_{\text{rod}} &= \frac{(1+s) V_{\text{rod}}}{V_{\text{ex\_rod}}} \\ &= \frac{(1+s)\frac{\pi}{4} D^2 L}{\frac{\pi}{2} D\left[\frac{\pi}{4} D^2 + L^2\right] + \frac{\pi}{4} D^2 L\,(3+\pi)}, \end{aligned} \qquad (5)$$

where s values are obtained empirically from simulation data, and Eq. (5) reduces to Eq. (3) in the slender-rod limit when $s = 0$. The reader should note that the quantity $1 + s = N_c V_{\text{ex\_rod}}$ is numerically equal to the average number of bonds or contacts per object at percolation B_c.[4,5] This follows from the fact that in an excluded volume framework, the critical number of bonds per object corresponds to the number of centers of objects that enter the excluded volume of a given object.[4] By definition, B_c (or $1 + s$) is also equivalent to the total excluded volume when the simulation volume is a unit cube. Using ϕ_c from our results and Eq. (5), calculated $(1 + s)$ values for $L/D = 10-100$ subsequently found (Fig. 1):

$$s = 3.2\left(\frac{R}{L}\right)^{0.46} \qquad (6)$$

Equation (6) gives the empirical correction factor for predicting ϕ_c for isotropic, monodisperse, soft-core rods with arbitrary L and D using the finite-L/D-excluded volume solution Eq. (5). Equation (6) is in good agreement with Berhan and Sastry's[5] expression $s = 5.23(L/R)^{-0.57}$, further corroborating our simulation method (see Supplemental Material Fig. 2).[20]

In Fig. 2, we compare the L/D dependence of the percolation threshold from our experimental silver nanowire–polystyrene composites[11] to (i) results from our simulations of monodisperse, isotropic networks of soft-core cylinders,[11] (ii) the excluded volume model slender-rod solution[4] [Eq. (3)], and (iii) the finite-L/D-excluded volume model solution [Eq. (5)] using values from our simulations [Eq. (6)]. Quantitative comparison of our simulations and model to experiments is credible because our silver nanowire–polystyrene composites meet the following important criteria: nanowires have narrow size dispersity and well-defined electrical properties, are straight cylinders, and are well dispersed in the polymer matrix.[11] The slender rod limit solution significantly underestimates ϕ_c relative to our experimental and simulation values, and this discrepancy is more pronounced for lower L/D values. On the other hand, there is reasonable agreement between

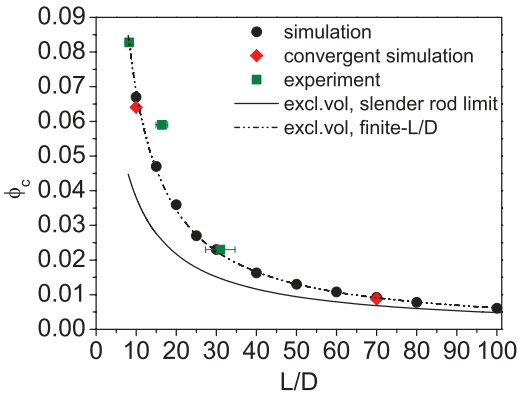

FIG. 2. (Color online) ϕ_c of monodisperse, isotropic, soft-core, cylindrical rod networks as a function of aspect ratio. Results from simulations (black circles and red diamonds), experimental silver nanowire–polystyrene nanocomposites[11] (green squares), excluded volume theory in the slender rod limit, Eq. (3) (solid line), and our finite-L/D-excluded volume solution [Eqs. (5) and (6)] (dotted line).

the experimental values and results from our simulations of soft-core, finite-sized cylindrical rods. Finally, ϕ_c predictions from our finite-L/D analytical solution are in excellent agreement with our simulation data, showing that Eqs. (5) and (6) are successful in extending the applicability of the excluded volume solution to networks of soft-core, monodisperse rods with finite L/D. In our earlier publication,[11] we highlighted the agreement between the simulations and experiments in Fig. 2. Here, we have made the critical advance of providing an analytical expression that captures the simulation and experimental results. This excluded volume theory for finite-size cylinders serves as the foundation from which we explore the impact of size dispersity in isotropic systems.

We propose a valuable extension to our finite-L/D-excluded volume model solution to predict ϕ_c for isotropic networks of rods with arbitrary distributions in L and D. We accomplished this by a heuristic generalization of the monodisperse case by taking the average of Eq. (5), with the assumption that L and D distributions are independent:

$$\phi_c = \frac{(1+s_{\text{poly}})\frac{\pi}{4}\langle D^2\rangle_n\langle L\rangle_n}{\frac{\pi}{2}\langle D\rangle_n\left[\frac{\pi}{4}\langle D^2\rangle_n+\langle L^2\rangle_n\right]+\frac{\pi}{4}\langle D^2\rangle_n\langle L\rangle_n(3+\pi)} = \frac{(1+s_{\text{poly}})}{\frac{\pi}{2}\frac{\langle D\rangle_n}{\langle L\rangle_n}+2\frac{\langle L\rangle_w}{\langle D\rangle_w}+(3+\pi)}, \tag{7a}$$

Furthermore, we use Eq. (6) from our monodisperse simulations to calculate s_{poly} as a function of the number average of L and R of the polydisperse rods.

$$s_{\text{poly}} = 3.2\left(\frac{\langle R\rangle_n}{\langle L\rangle_n}\right)^{0.46} \tag{7b}$$

The first term in the denominator of Eq. (7a) is negligibly small at low L/D and vanishes as L/D increases; thus, the expression is dominated by the weight average term in the denominator. The result is a weight average dependence of the percolation threshold on the rod dimension distributions and is in qualitative agreement with the infinite-L/D analytical solutions by van der Schoot and co-workers.[13–15] A weight average dependence is intuitive, since higher L/D rods in the polydisperse network play a more critical role in network expansion. Experimentally, where the exact form of the size distributions may not be known, the sample mean and variance suffice to estimate the first and second moments of L and R distributions in Eqs. (7). The generalization of the $(1+s)$ correction factor in Eq. (7b) involves a number average because the quantity $(1+s)=B_c$, or the total excluded volume, is proportional to the number density of rods at percolation, Eq. (4). Thus, as expected, calculating $(1+s_{\text{poly}})$ based on the weight average of the rod dimensions resulted in a poorer fit to simulation data, particularly for large size distributions (see Supplemental Material Fig. 5).[20]

First, we compare our analytical expression [Eqs. (7)] to simulations of rods having experimentally relevant Gaussian distributions in L and D. In Fig. 3, we plot simulation results and generalized model [Eqs. (7)] predictions of the effect of Gaussian distributions of varying width on the percolation threshold for rod networks that have polydispersity in L only, D only, or both L and D. For wide distributions ($\sigma_L, \sigma_D > 30\%$ of L_{mode}, D_{mode}), we truncate negative values

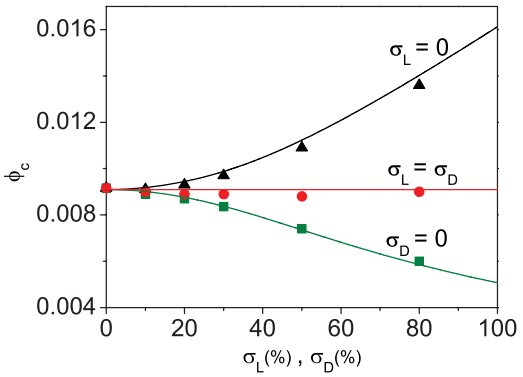

FIG. 3. (Color online) Simulation data (points) with corresponding generalized excluded volume predictions [Eqs. (7), lines] for ϕ_c in networks where rods have a Gaussian distribution in length (green squares), diameter (black triangles), or both (red circles). The width of the respective distributions is given by the standard deviation, σ_L or σ_D, which is expressed as a percentage of L_{mode} (0.04 units) or D_{mode} (0.00057143 units), and $L_{\text{mode}}/D_{\text{mode}} = 70$.

of L and D, breaking the symmetry of the Gaussian distribution and resulting in an excess of longer ($L_{\text{mode}} < \langle L\rangle_n < \langle L\rangle_w$) or wider rods ($D_{\text{mode}} < \langle D\rangle_n < \langle D\rangle_w$). Figure 3 shows that ϕ_c is insensitive to polydispersity for narrow distributions ($\sigma_L, \sigma_D < 30\%$) and when size polydispersity is comparable in both L and D ($\sigma_L = \sigma_D$). On the other hand, a significant decrease in ϕ_c relative to the monodisperse case is observed for large dispersities in L when $\sigma_D = 0$ because of the abovementioned asymmetry of the L distribution that results in an excess of longer high-L/D rods. Conversely, large dispersities in D when $\sigma_L = 0$ cause ϕ_c to increase due to an excess of wider low-L/D rods. Moreover, we also observe excellent agreement between our simulations and predictions from our generalized excluded volume model solution [Eqs. (7)] for polydisperse rod networks. Similar results were obtained for rod networks with a lower $L_{\text{mode}}/D_{\text{mode}} = 10$ (see Supplemental Material).[20]

Second, we explore the effect of bidisperse distributions in rod size on isotropic networks comprising two size populations, namely low- and high-aspect-ratio rods. These networks exploit the dominant contribution of high-L/D filler particles in network formation and the processability of low-L/D particles. Similar networks were studied by van der Schoot and co-workers[13–15] for rods with infinite L/D and by Rahatekar *et al.*,[27] who simulated the effects of small additions of low-L/D rods to oriented networks of high-L/D rods. To simulate a bidisperse network morphology, we define reference rods with $L/D = 10$ ($L_{\text{Ref}} = 0.04$ units, $D_{\text{Ref}} = 0.004$ units), and longer high-L/D rods ($L > L_{\text{Ref}}$, $D = D_{\text{Ref}}$), where the rod length ratio is $r_L = L_{\text{Long}}/L_{\text{Ref}}$. The amount of longer rods added to the network is given as a relative volume fraction $F_{\text{Long}} = \phi_{\text{Long}}/(\phi_{\text{Long}} + \phi_{\text{Ref}})$. By increasing F_{Long}, ϕ_c is lowered and the reduction in ϕ_c is most pronounced at small F_{Long} for larger r_L, Fig. 4(a). We also observe excellent agreement between our simulations and predictions from our generalized excluded volume model expression [Eqs. (7)], showing that the solution holds for arbitrary distributions in L and D. Similar results were obtained for rods with a

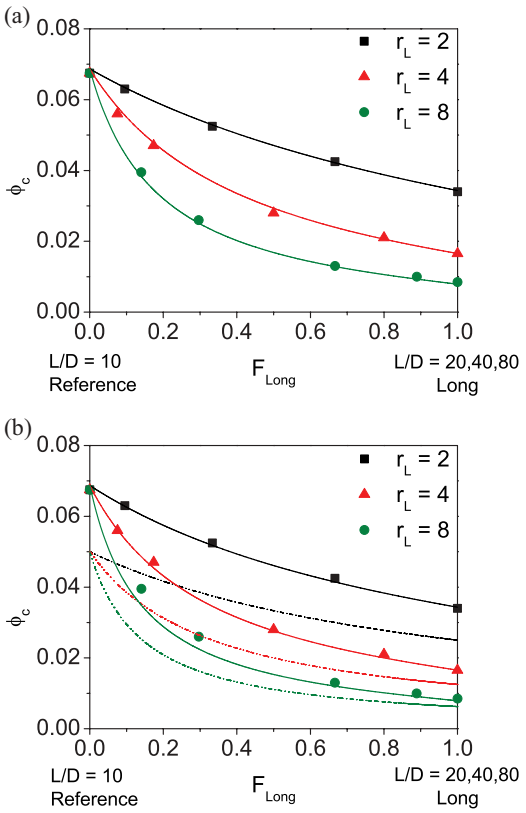

FIG. 4. (Color online) (a) Simulation (points) and generalized excluded model predictions [Eqs. (7), lines] for ϕ_c of bidisperse rod networks versus the relative volume fraction of longer rods in the system (F_{Long}) for rod length ratios $r_L = 2, 4$, and 8, where $L_{\text{Ref}} = 0.04$ units and $D = 0.004$ units (constant). (b) Simulation (points) and corresponding ϕ_c predictions from Otten and van der Schoot's analytical model, as published [Eq. (8)] (dashed lines) and calibrated [Eq. (9)] (solid lines). ϕ_c predictions a function of F_{Long} for $r_L = 2$, 4, and 8.

bidisperse distribution in diameter, with the higher L/D rods in the bidisperse system being thinner ($D < D_{\text{Ref}}$, $L = L_{\text{Ref}}$) and $F_{\text{Thin}} = \phi_{\text{Thin}}/(\phi_{\text{Thin}} + \phi_{\text{Ref}})$ (Supplemental Material).[20] Note that others use a number fraction notation (x) and report a very dramatic reduction in ϕ_c for small x_{Long}, versus a moderate effect for large x_{Thin}.[14] We report bidispersity in volume fraction because the volume of rods depends differently on L and D ($V \propto D^2$ vs $V \propto L$), and volume fraction is experimentally more accessible than number fraction.

For completeness, we consider the analytical model of Otten and van der Schoot for the case of soft-core, finite-L/D, polydisperse rod networks. In their comprehensive theoretical study,[14,15] they use tools from both percolation and liquid state theories to formulate a general analytical expression for the percolation threshold for polydisperse cylindrical fillers in the slender-rod limit ($L/D \to \infty$). For ideal (soft-core) rods, their slender-rod limit solution for the ϕ_c of rods with arbitrary distributions in L and D is:

$$\phi_{c,\text{Otten}} = \frac{\langle D^2\rangle_n}{\langle L\rangle_w(\langle D\rangle_n + \sqrt{\langle D^2\rangle_n})} \tag{8}$$

We perform a series of calibrations on this solution to adapt it to polydisperse networks of finite-L/D rods. First, we calibrate their monodisperse result in the slender-rod limit, $\phi_c = D/2L$, against the corresponding excluded volume result [Eq. (3)], which has been proven to be exact in this regime.[6,7] We then apply the $(1 + s)$ factor from our simulations for finite-sized monodisperse cylinders [Eq. (6)]. Finally, we generalize the calibration factor from the finite-L/D monodisperse case to polydisperse rod networks by taking the respective number averages, yielding a calibrated version of Otten and van der Schoot solution for isotropic, finite-L/D rod networks with arbitrary distributions in L and D:

$$\phi_{c,\text{Otten calib}} = c \times \frac{\langle D^2\rangle_n}{\langle L\rangle_w(\langle D\rangle_n + \sqrt{\langle D^2\rangle_n})},$$
$$c = \frac{(1 + s_{\text{poly}})}{\frac{\pi}{4}\frac{\langle D^2\rangle_n}{\langle L^2\rangle_n} + \frac{(3+\pi)}{2}\frac{\langle D\rangle_n}{\langle L\rangle_n} + 1} \tag{9}$$

Equation (9) shows the same weight average dependence on L as our generalized excluded volume theory [Eqs. (7)], but their dependencies on D differ slightly. In Fig. 4(b), we compare ϕ_c results from our simulations, the as-published Otten and van der Schoot model [Eq. (8)], and the calibrated Otten and van der Schoot model [Eq. (9)] for rod networks with bidispersity in length. Their as-published solution [Eq. (8)] significantly underestimates ϕ_c of the bidisperse network relative to our simulations of finite-L/D cylindrical rods, and the extent of this underestimation is more pronounced at lower F_{Long} when the mean L/D of the rod ensemble is smaller. In contrast, there is very good agreement between our simulations and our calibration of the Otten and van der Schoot model [Eq. (9)]. Note that fits to the simulation data are comparable for our generalized excluded volume expression [Eqs. (7)] and the calibrated Otten and van der Schoot model [Eq. (9)].

IV. CONCLUSIONS

We have simulated three-dimensional isotropic networks of finite, soft-core, conductive cylinders with Gaussian and bidisperse distributions in their length and diameter. We have also generalized the popular excluded volume model of percolation, which was originally formulated for soft-core, infinite-L/D, monodisperse rod networks, to account for finite-L/D and polydisperse rod sizes. Finally, we adapted Otten and van der Schoot's analytical model for polydisperse rods in the slender-rod limit,[14,15] successfully extending its applicability to polydisperse networks of soft-core rods with modest L/D. For arbitrary distributions in L and D of cylindrical rods, we obtain a weight average dependence of ϕ_c on the filler dimensions, an intuitive result since higher L/D rods are more critical in network expansion. Following from the good agreement between our monodisperse simulation predictions and experimental thresholds from silver nanowire–polystyrene composites[11] (Fig. 2), coupled with the demonstrated inaccuracy of popular slender-rod-limit analytical models for fillers with L/D as high as 500,[5] our simulation results and generalized excluded volume model for polydisperse rods of finite L/D [Eqs. (7)] provide experimentalists with a robust

and convenient toolkit for designing and evaluating composites with finite-sized cylindrical nanofillers. In future work, we plan to extend our simulation method and generalized excluded volume model to address oriented networks of polydisperse rods.

ACKNOWLEDGMENTS

This work was supported primarily by the MRSEC program of the National Science Foundation under Award No. DMR-11-20901, and by the University Research Foundation of the University of Pennsylvania.

[1] I. Balberg and N. Binenbaum, Phys. Rev. B **28**, 3799 (1983).
[2] F. Du, J. Fischer, and K. Winey, Phys. Rev. B **72**, 121404(R) (2005).
[3] A. Behnam, J. Guo, and A. Ural, J. Appl. Phys. **102**, 044313 (2007).
[4] I. Balberg, C. H. Anderson, S. Alexander, and N. Wagner, Phys. Rev. B **30**, 3933 (1984).
[5] L. Berhan and A. Sastry, Phys. Rev. E **75**, 041120 (2007).
[6] A. L. R. Bug and S. A. Safran, Phys. Rev. B **33**, 4716 (1986).
[7] A. L. R. Bug, S. A. Safran, and I. Webman, Phys. Rev. Lett. **54**, 1412 (1985).
[8] M. Foygel, R. Morris, D. Anez, S. French, and V. Sobolev, Phys. Rev. B **71**, 104201 (2005).
[9] Z. Néda, R. Florian, and Y. Brechet, Phys. Rev. E **59**, 3717 (1999).
[10] S. I. White, B. A. DiDonna, M. Mu, T. C. Lubensky, and K. I. Winey, Phys. Rev. B **79**, 024301 (2009).
[11] S. I. White, R. M. Mutiso, P. M. Vora, D. Jahnke, S. Hsu, J. M. Kikkawa, J. Li, J. E. Fischer, and K. I. Winey, Adv. Funct. Mater. **20**, 2709 (2010).
[12] W. Bauhofer and J. Z. Kovacs, Compos. Sci. Technol. **69**, 1486 (2009).
[13] A. V. Kyrylyuk and P. van der Schoot, Proc. Natl. Acad. Sci. USA **105**, 8221 (2008).
[14] R. H. J. Otten and P. van der Schoot, Phys. Rev. Lett. **103**, 225704 (2009).
[15] R. H. J. Otten and P. van der Schoot, J. Chem. Phys. **134**, 094902 (2011).
[16] A. P. Chatterjee, J. Chem. Phys. **132**, 224905 (2010).
[17] A. P. Chatterjee, J. Stat. Phys. **146**, 244 (2012).
[18] B. P. Grady, Macromol. Rapid Commun. **31**, 247 (2010).
[19] M. R. Hestenes and E. Stiefel, J. Res. Natl. Bur. Stand. **49**, 409 (1952).
[20] See Supplemental Material at http://link.aps.org/supplemental/10.1103/PhysRevB.86.214306 for simulation results.
[21] I. Balberg, Phys. Rev. Lett. **59**, 1305 (1987).
[22] I. Balberg, J. Phys. D: Appl. Phys. **42**, 064003 (2009).
[23] C. Grimaldi and I. Balberg, Phys. Rev. Lett. **96**, 066602 (2006).
[24] N. Johner, C. Grimaldi, I. Balberg, and P. Ryser, Phys. Rev. B **77**, 174204 (2008).
[25] S. Vionnet-Menot, C. Grimaldi, T. Maeder, S. Strässler, and P. Ryser, Phys. Rev. B **71**, 064201 (2005).
[26] L. Onsager, Ann. N.Y. Acad. Sci. **51**, 627 (1949).
[27] S. S. Rahatekar, M. S. P. Shaffer, and J. A. Elliott, Compos. Sci. Technol. **70**, 356 (2010).